Inelastic scattering of fast neutrons from excited states in ^{56}Fe

R. Schwengner, R. Beyer, A.R. Junghans, R. Massarczyk, M. Anders, D. Bemmerer, A. Ferrari, R. Hannaske, T. Kögler, M. Röder, K. Schmidt, A. Wagner

Institute of Radiation Physics, Helmholtz-Zentrum Dresden-Rossendorf, 01328 Dresden, Germany

HZDR

HELMHOLTZ ZENTRUM DRESDEN ROSSENDORF

Setup at nELBE

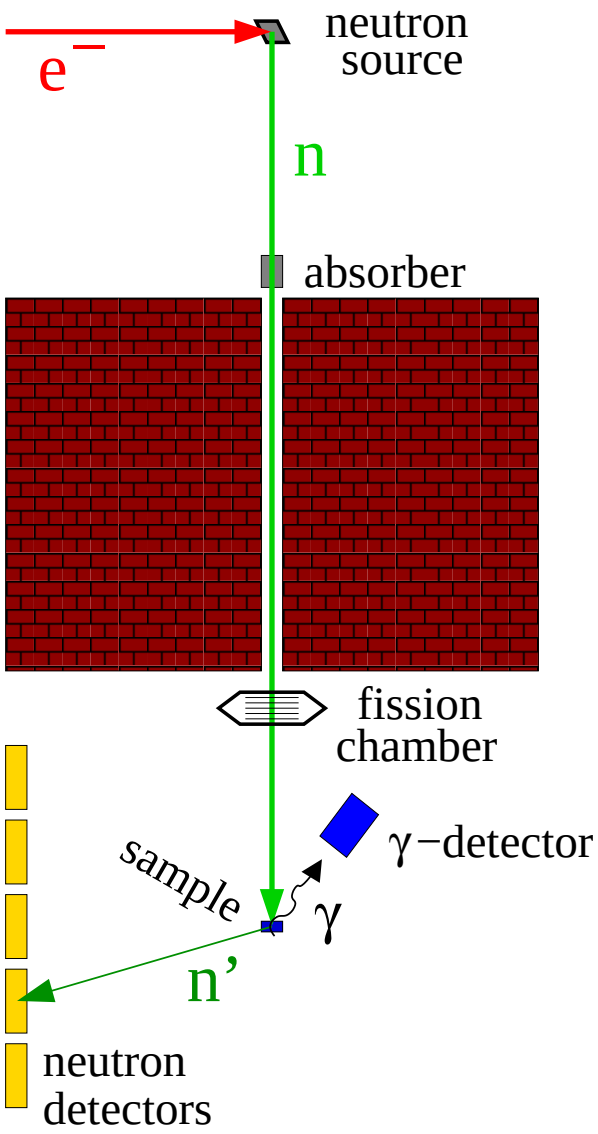

- Target: cylinder of natural iron diameter 20 mm, thickness 8 mm
- HPGe detector at 125° to the neutron beam and a distance of 20 cm from the target
- Time difference between accelerator pulse and signal of the HPGe detector
  ⇒ time-of-flight of the incident neutrons
  ⇒ time resolution 10 ns

Neutron-scattering cross section

$$\sigma(E_i) = \frac{N_\gamma(E_n)}{\varepsilon(E_\gamma)\Delta E_{n,\gamma}} \cdot \left[\frac{\Phi(E_n)}{\Delta E_{n,\Phi}} N_{\mathrm{at}}\right]^{-1}$$

$\sigma(E_i)$ – scattering cross section of the state at the excitation energy E_i.
$N_\gamma(E_n)$ – number of events in the γ peak observed at a neutron energy E_n.
$\varepsilon(E_\gamma)$ – absolute efficiency of the HPGe detector at the transition energy E_γ.
$\Delta E_{n,\gamma}$ – neutron-energy bin width deduced from the gate width in the time-of-flight spectrum.
$\Phi(E_n)$ – neutron fluence (time integral over the neutron flux) at E_n.
$\Delta E_{n,\Phi}$ – neutron-energy bin width of the neutron fluence.
N_{at} – number of atoms per target area.

Gamma-ray spectra at various neutron energies

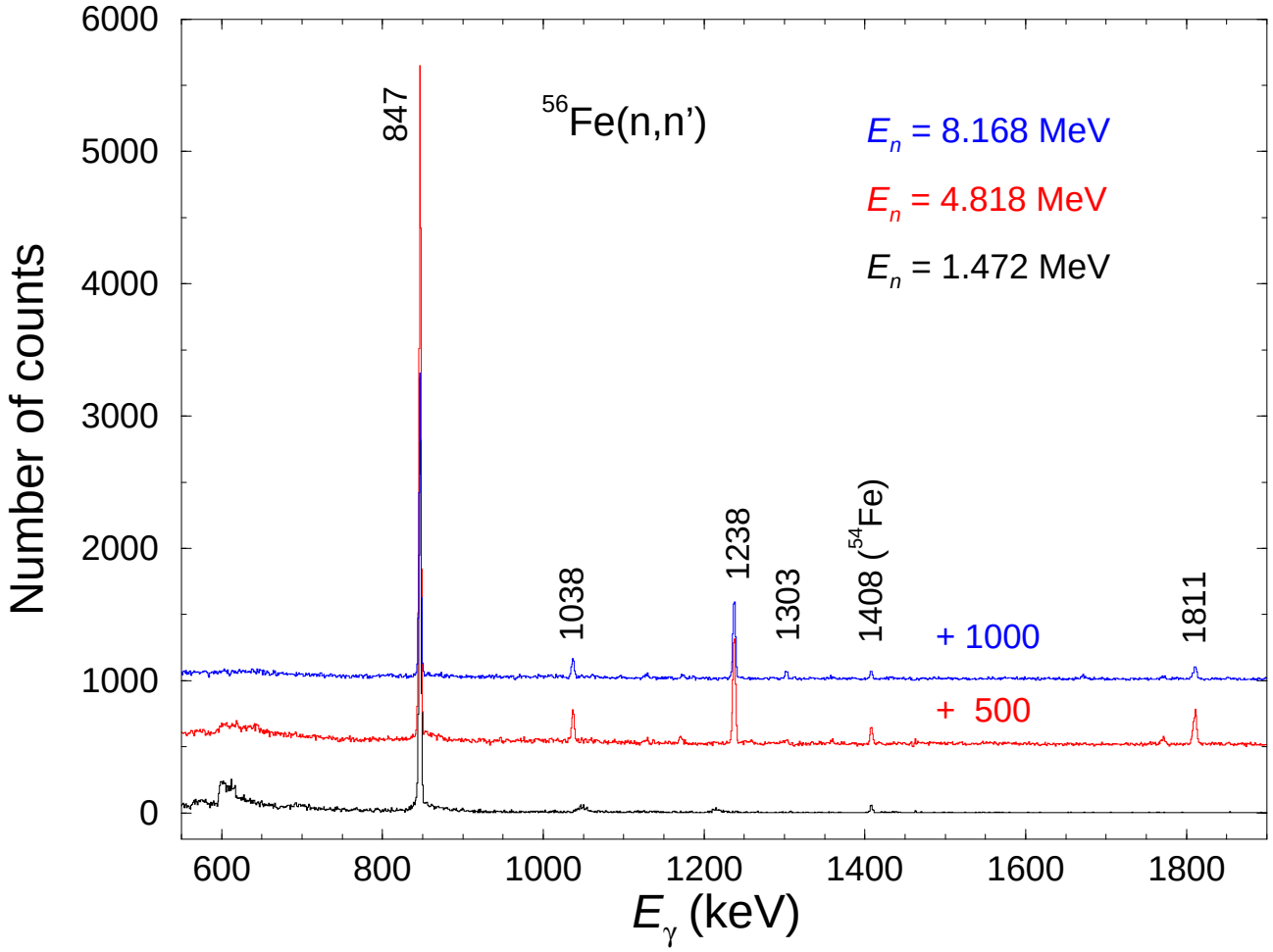

Neutron fluence

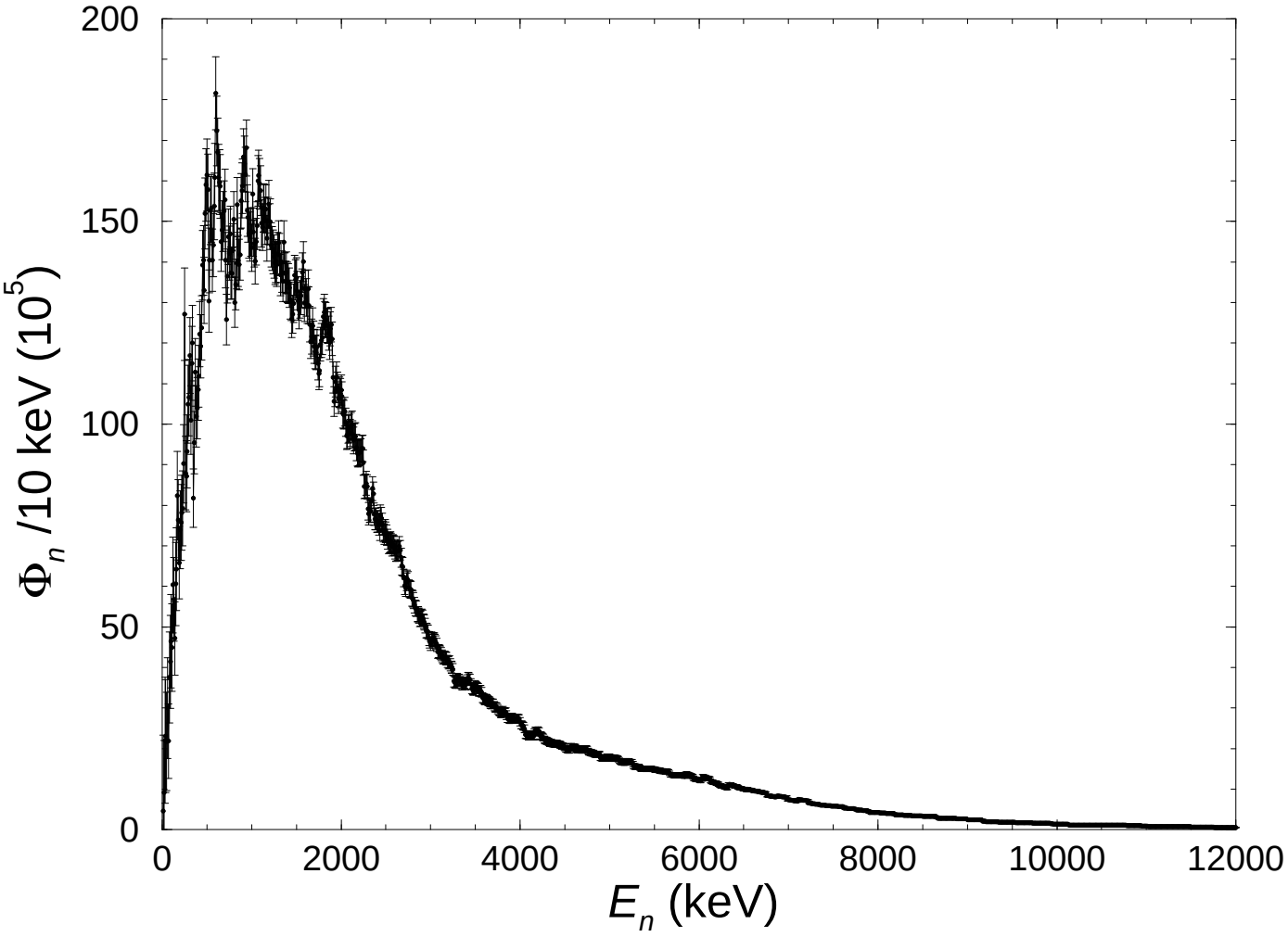

Neutron fluence measured by means of a fission chamber of PTB Braunschweig as described in R. Beyer et al., NIM A 723, 151 (2013).

Multiple inelastic scattering from ^{56}Fe

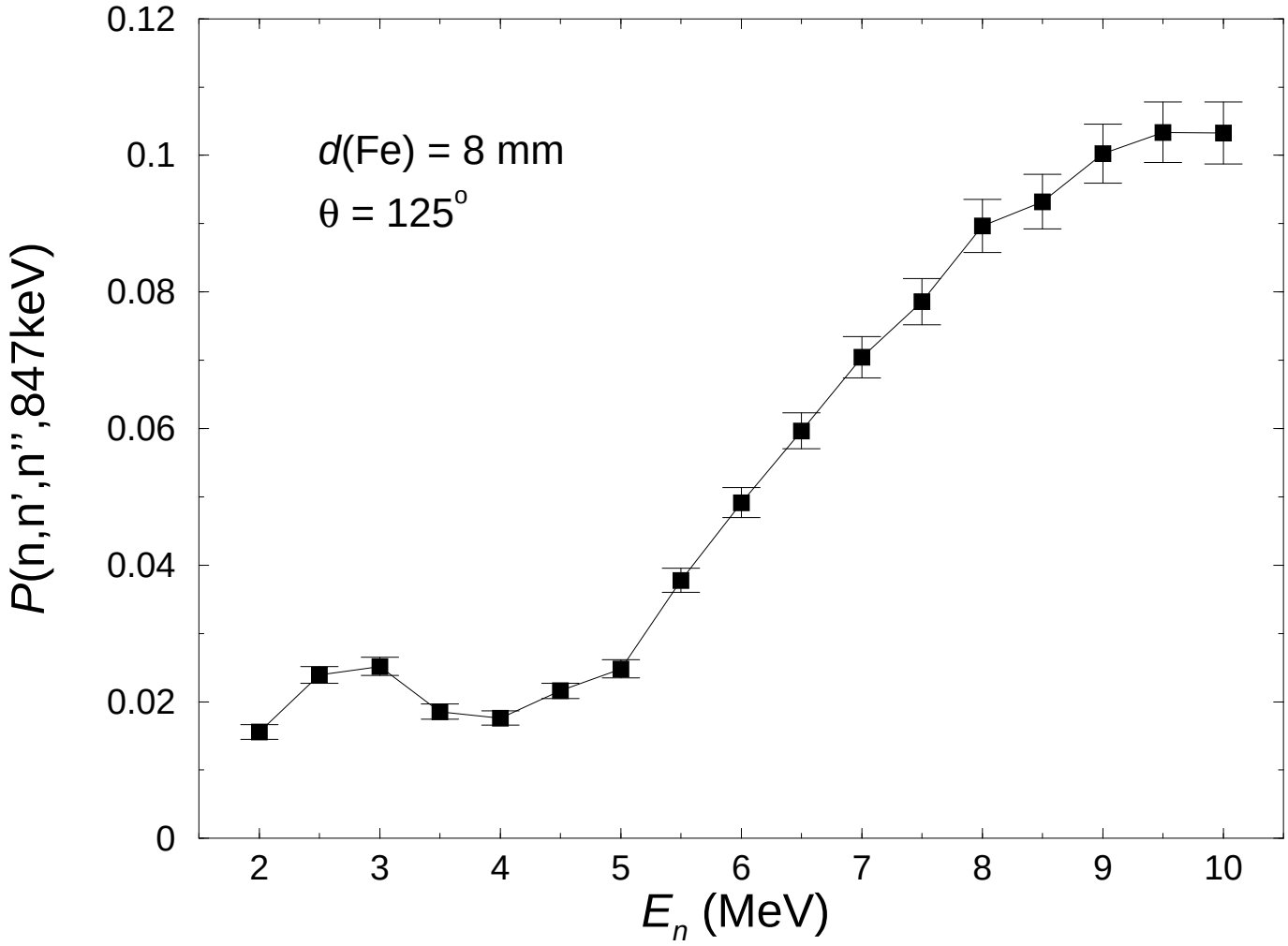

Excitation of 2^+ states in two ^{56}Fe nuclei by one neutron and detection of the 847 keV γ rays at 125°.

Excited states in ^{56}Fe

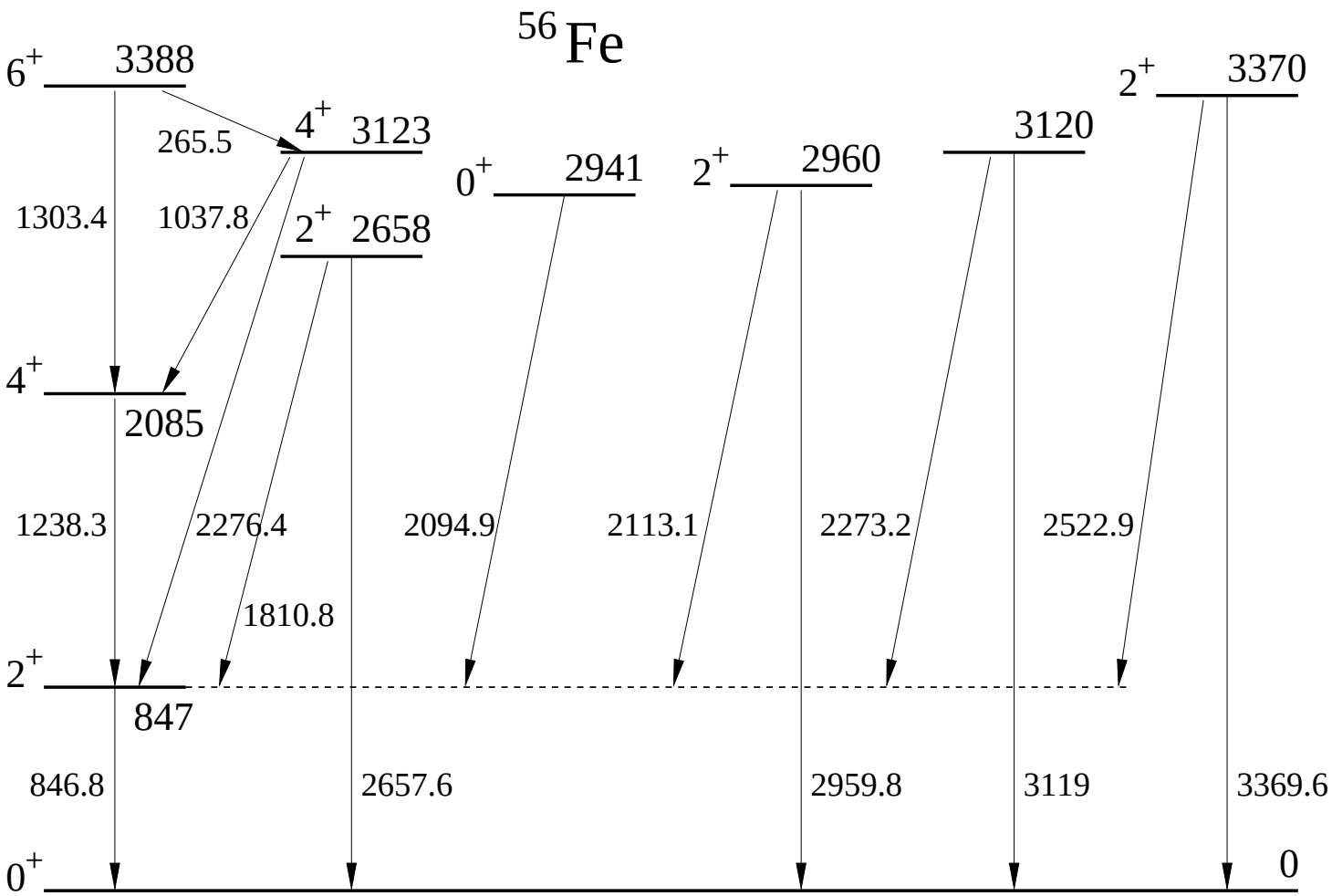

Cross sections of inelastic scattering from ^{56}Fe

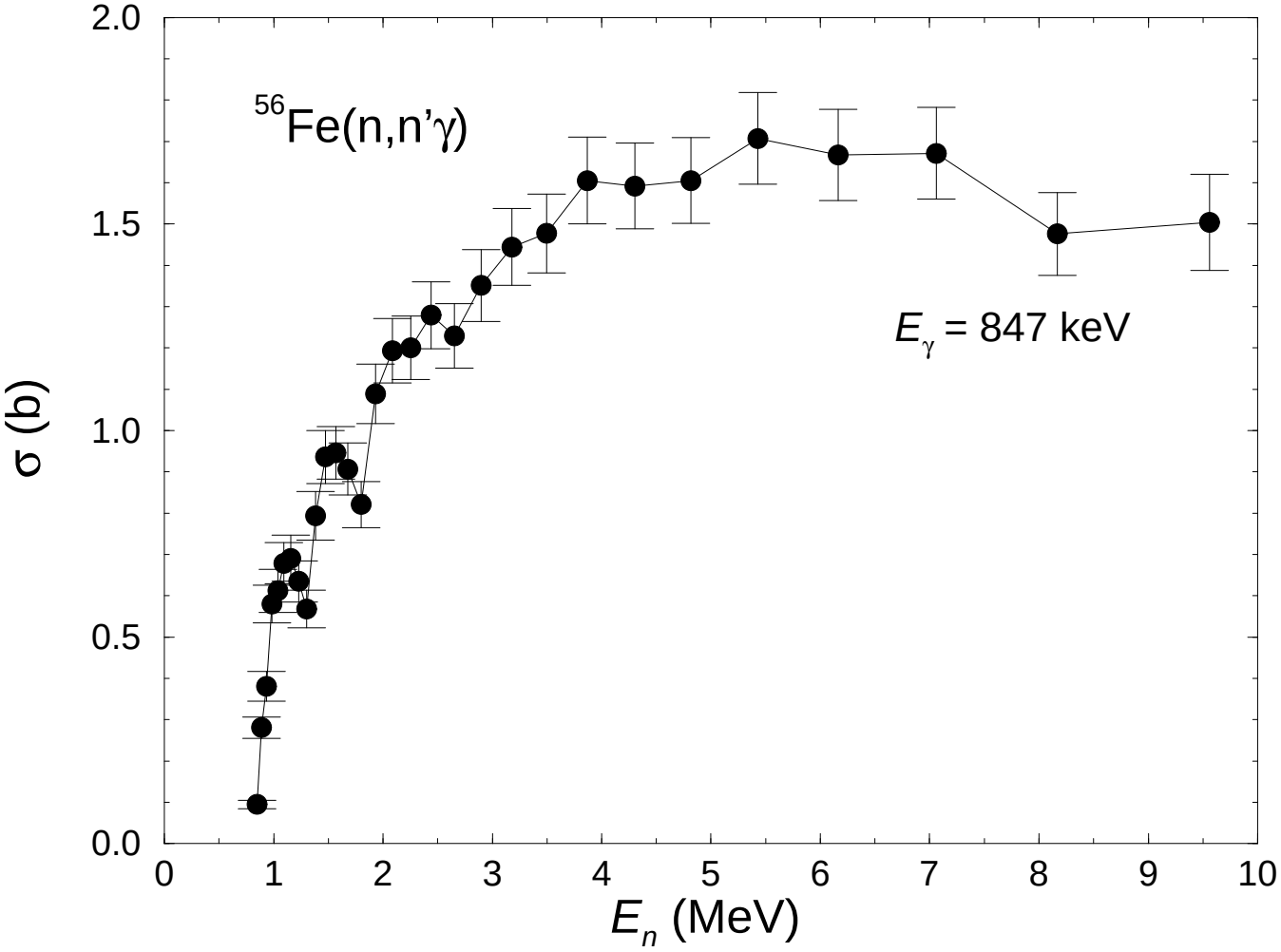

Total scattering cross section of ^{56}Fe deduced from the $2_1^+ \rightarrow 0_1^+$ transition at 847 keV.

Cross sections of inelastic scattering from ^{56}Fe

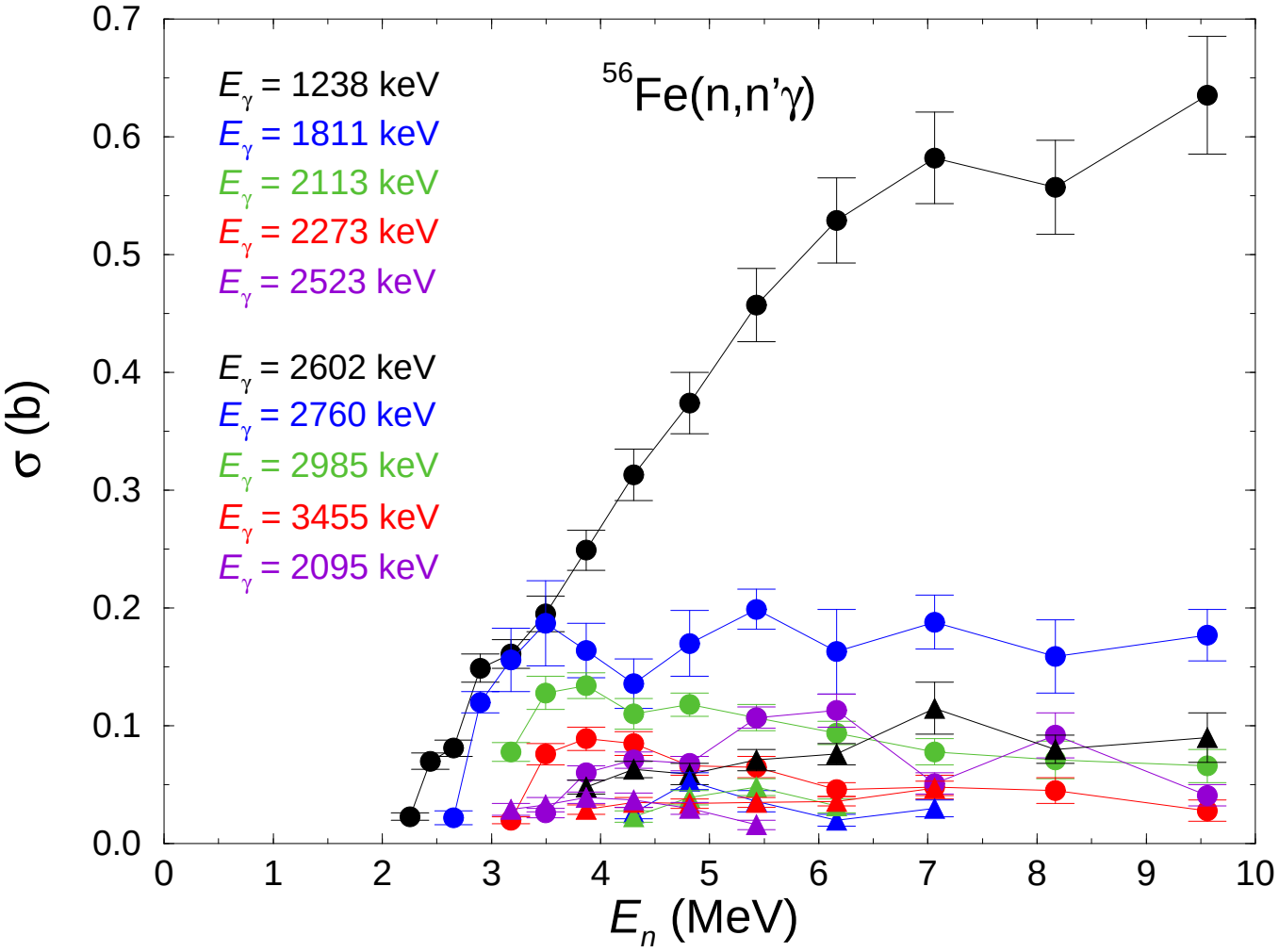

Scattering cross sections of states feeding the 2_1^+ state at 847 keV.

Cross sections of inelastic scattering from ^{56}Fe

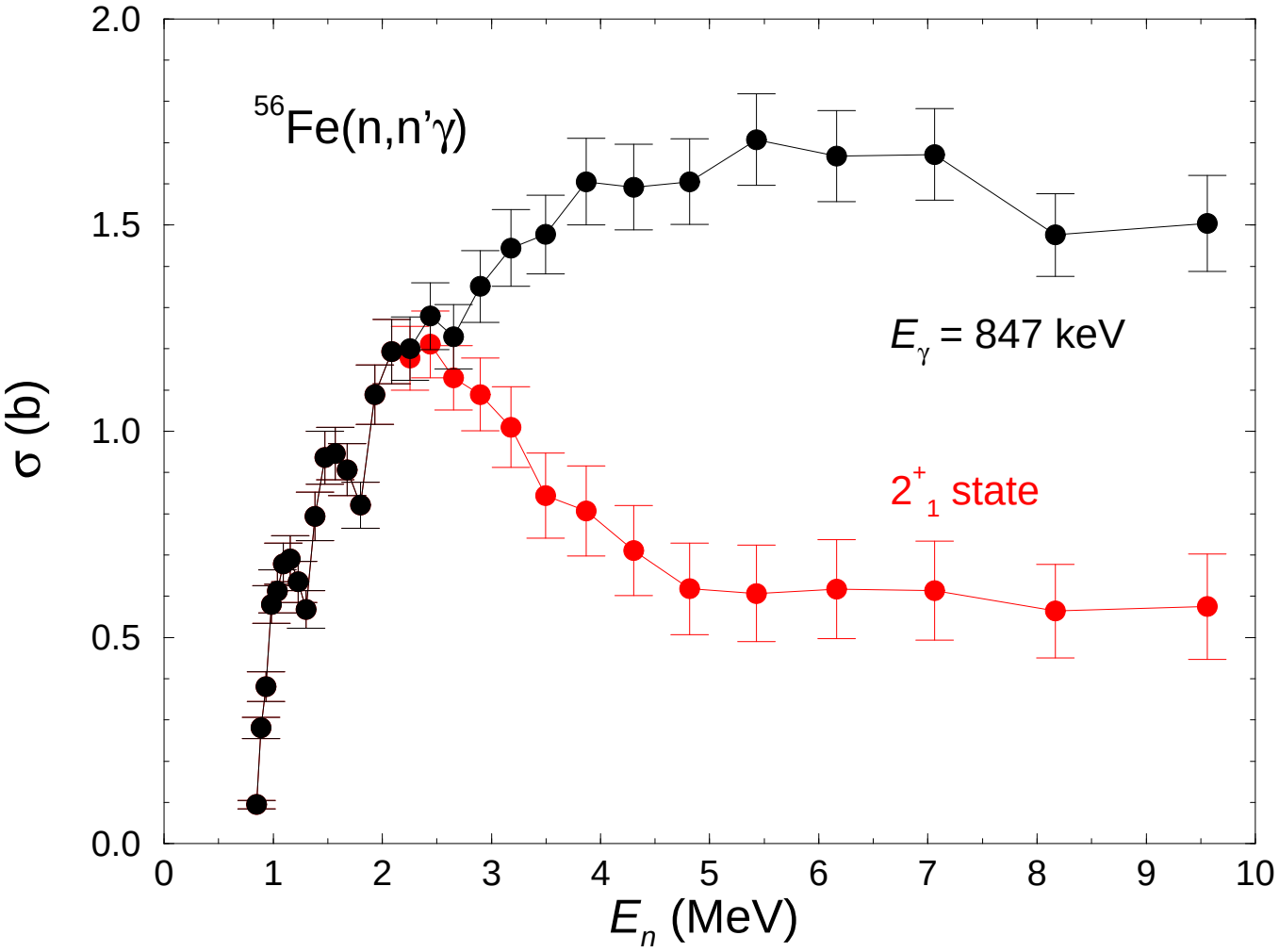

Total scattering cross section of ^{56}Fe and cross section of the 2^+_1 state resulting from the feeding correction.

Cross sections of inelastic scattering from ^{56}Fe

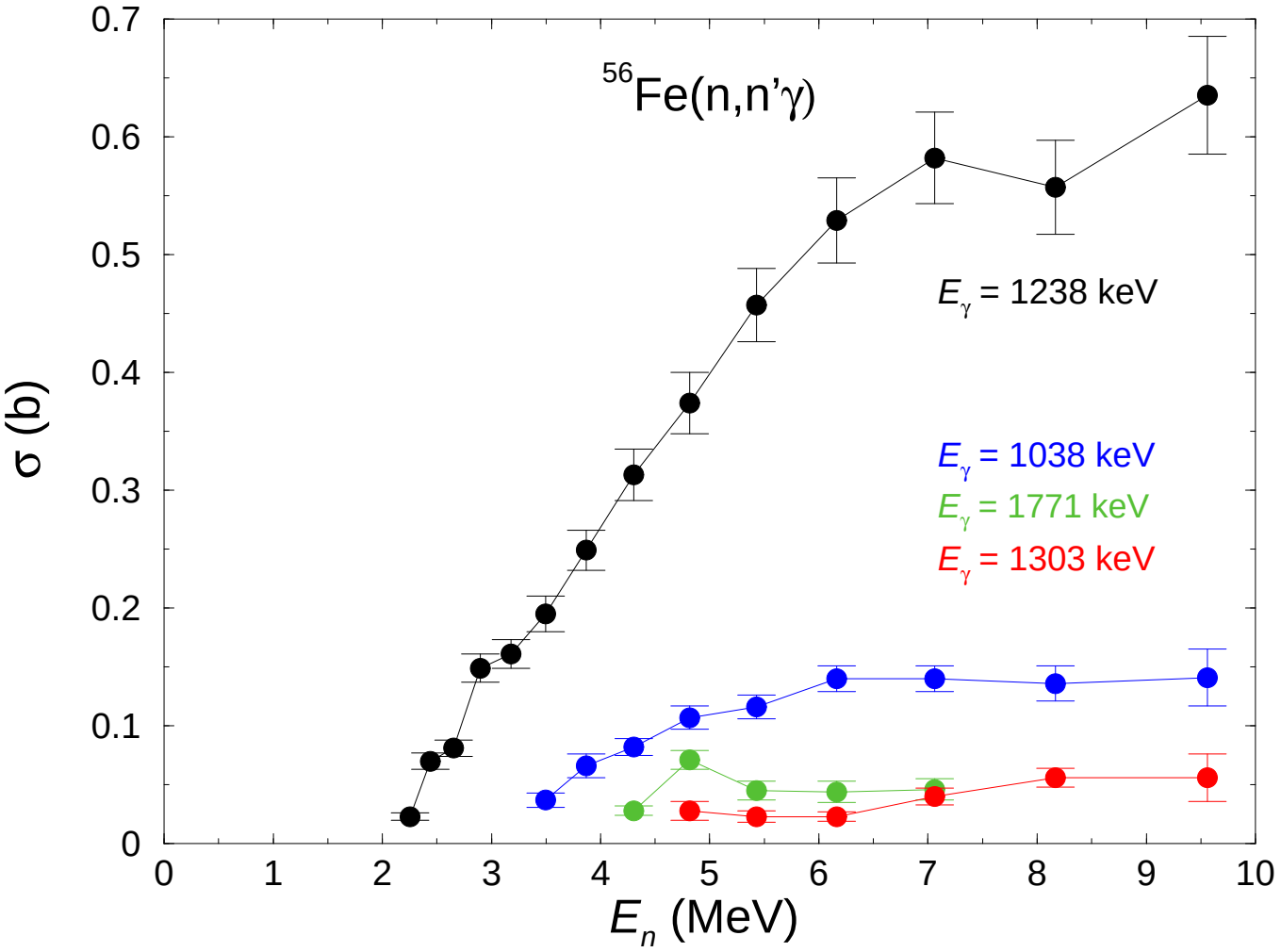

Scattering plus feeding cross section of the 4_1^+ state and cross sections of feeding states.

Cross sections of inelastic scattering from ^{56}Fe

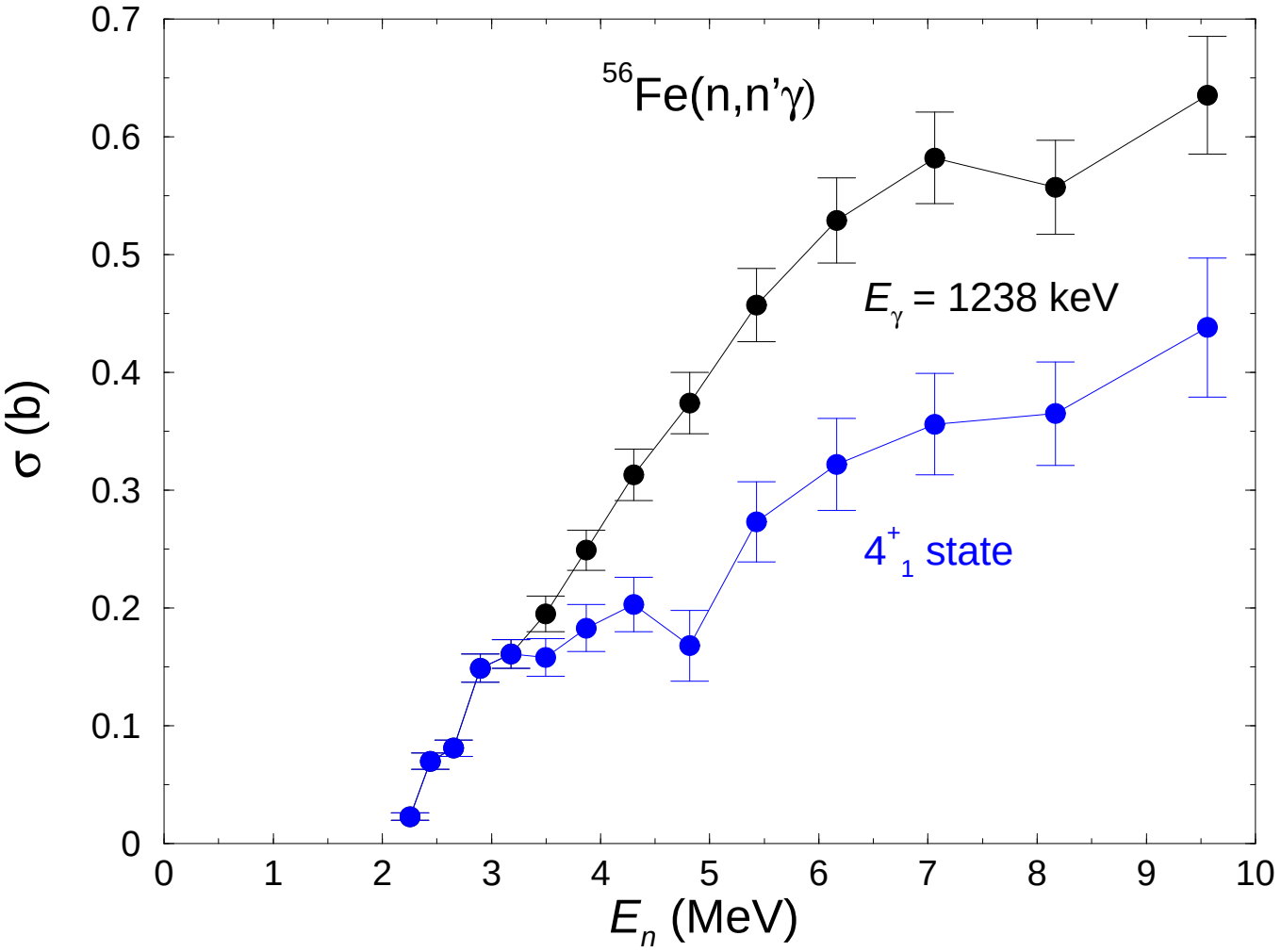

Scattering cross section deduced from the 1238 keV transition and cross section of the 4^+_1 state resulting from the feeding correction.

Cross sections of inelastic scattering from ^{56}Fe

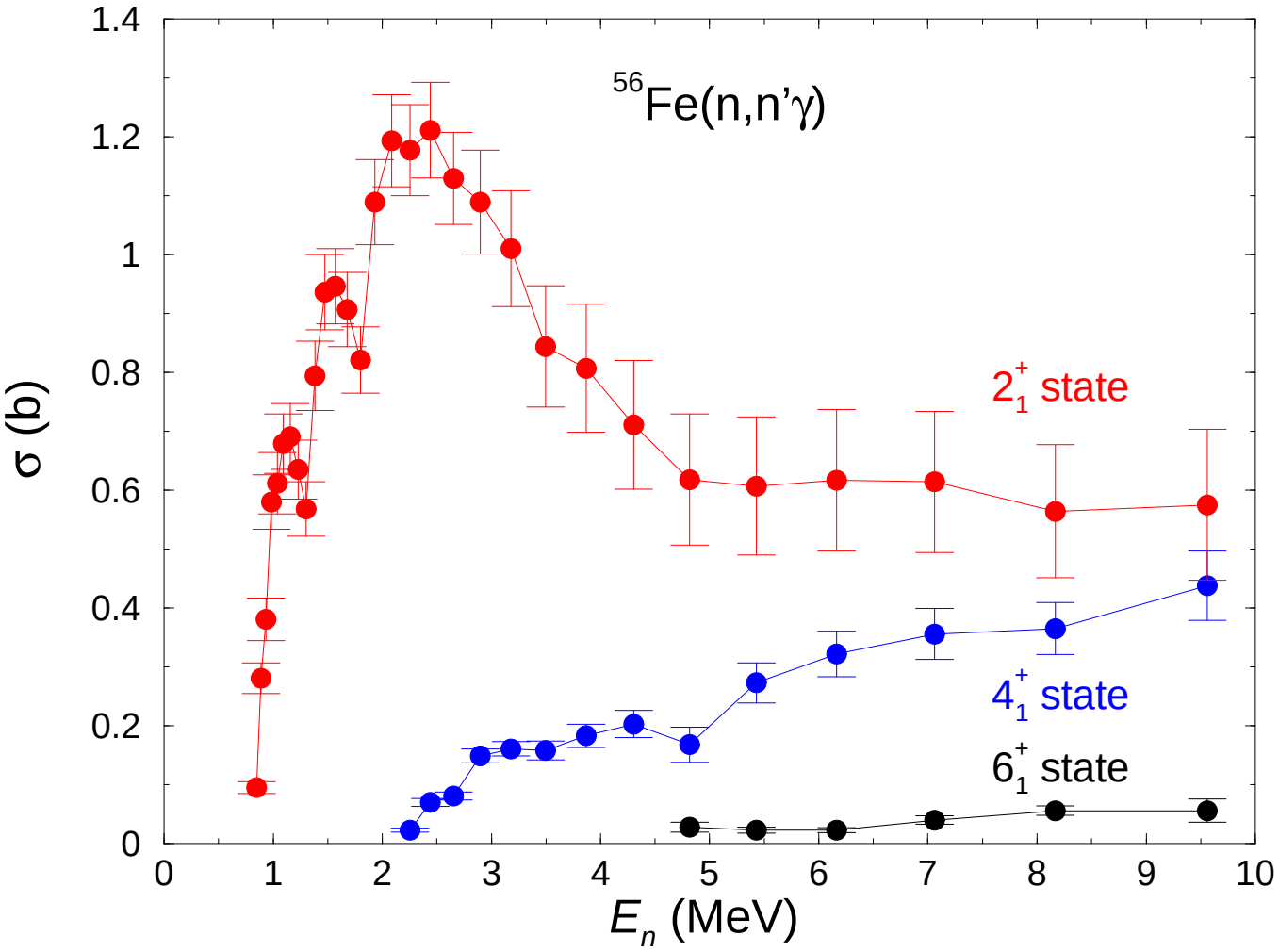

Scattering cross sections of the 2_1^+, 4_1^+ and 6_1^+ states.

Cross sections of inelastic scattering from ^{56}Fe

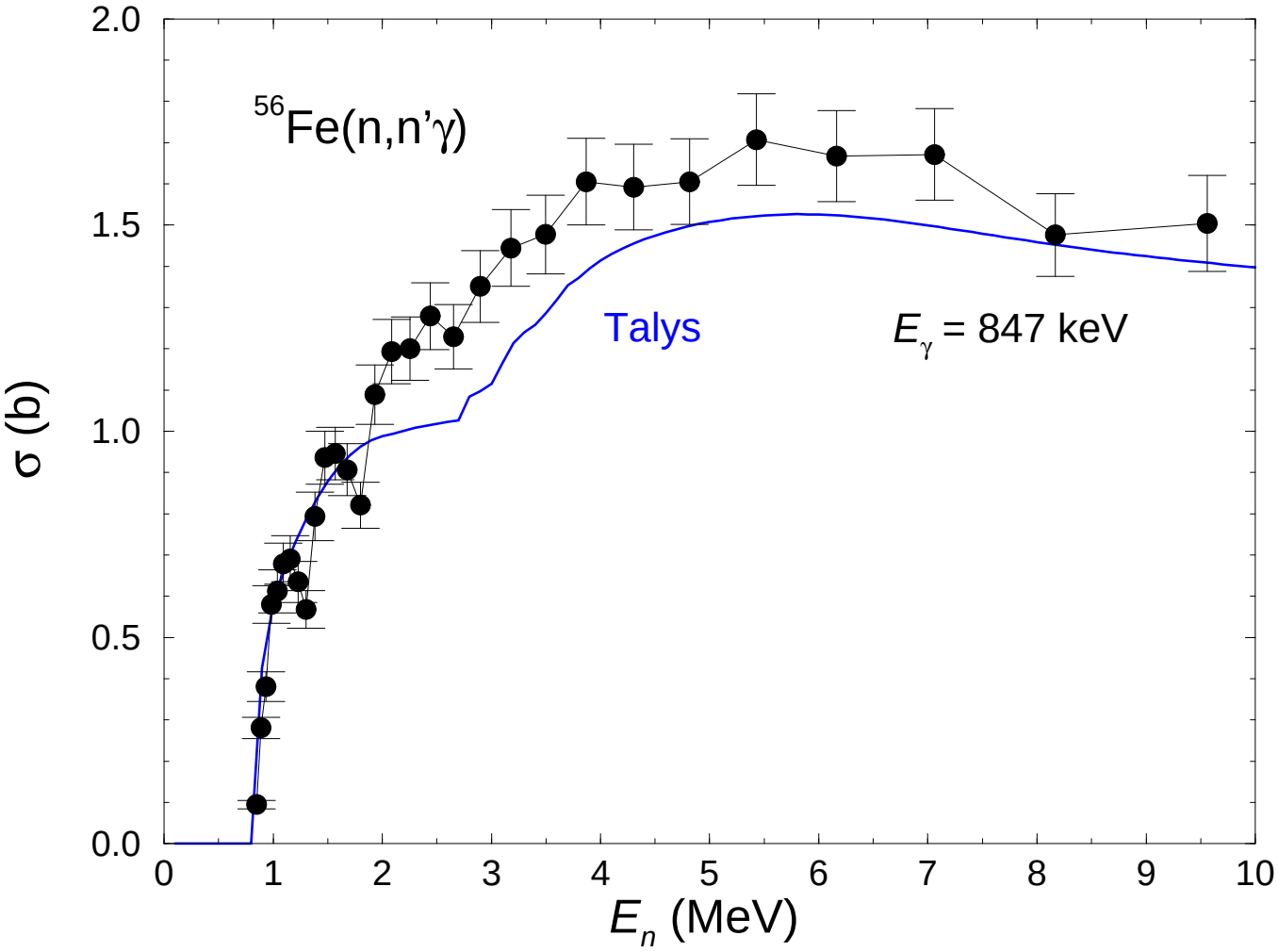

Total scattering cross section of ^{56}Fe deduced from the $2_1^+ \rightarrow 0_1^+$ transition at 847 keV in comparison with Talys calculations.

Conclusions

- High-resolution measurement of γ rays from states excited in inelastic neutron scattering.
- Determination of the cross section for individual excited states as a function of the neutron energy.
- Advantage of the measurement of γ rays with an HPGe detector: measurement of the time-of-flight of the scattered neutrons not needed.
  Disadvantage: time resolution of 10 ns compared with 0.7 ns of the plastic scintillators used for the detection of scattered neutrons.
  $\Rightarrow$ Fine structures of the cross sections may be washed out.